Spectroscopic characterization and laser test of a 10*at.%* Yb:Y$_3$Sc$_{1.5}$Al$_{3.5}$O$_{12}$ ceramic sample

Angela Pirri[1], Guido Toci[2*], Jiang Li[3], Yagang Feng[3], Tengfei Xie[3], Zhaoxiang Yang[3], Barbara Patrizi[4], Matteo Vannini[2]

[1]*Istituto di Fisica Applicata "Carrara", Consiglio Nazionale delle Ricerche, IFAC-CNR,Via Madonna del Piano 10C, 50019 Sesto Fiorentino (Fi), Italy*
[2]*Istituto Nazionale di Ottica, Consiglio Nazionale delle Ricerche, INO-CNR,Via Madonna del Piano 10C, 50019 Sesto Fiorentino (Fi), Italy*
[3]*Key Laboratory of Transparent and Opto-functional Advanced Inorganic Materials, Shanghai Institute of Ceramics, Chinese Academy of Sciences, 1295 Dingxi Road, Shanghai 200050, China*
[4]*Istituto Nazionale di Ottica, Consiglio Nazionale delle Ricerche, INO-CNR, Largo Fermi 6, 50125 Firenze, Italy*

*Corresponding author: Tel: (+39) 055-5225315; E-mail: guido.toci@ino.cnr.it

Abstract

We present the spectroscopic characterization and the laser measurements obtained with a 10 *at.%* Yb:Y$_3$Sc$_{1.5}$Al$_{3.5}$O$_{12}$ (=YSAG) ceramic sample. Longitudinally pumped in *quasi*-Continuous Wave (QCW) and in Continuous Wave (CW) at 936 nm, the ceramic has shown good laser performance. In the former pumping regime it delivers 6.7 W with a slope efficiency of η_s=67.8% and a laser threshold below 0.5 W. In the latter, the maximum output power was 5 W with η_s=52.7%. Finally, the tunable laser action has been obtained in the range between 991.5 nm and 1073 nm, *i.e.* 81.5 nm, by using a ZnSe prism. Copyright © 2019 VBRI Press.

Keywords: Solid state laser, transparent laser ceramic, ytterbium-doped laser ceramics, diode-pumped solid-state laser, tunable laser cavity.

Introduction

Y$_3$Sc$_x$Al$_{(1-x)}$O$_{12}$ (= YSAG) host is a disordered matrix (available as crystals [**1, 2**] or ceramics [**3**]) suitable for the development of laser devices with tunable emission or to generate short laser pulses [**4, 5**]. The main reasons underpinning these uses are, first, an emission spectrum of Yb^{3+} that is wider than in other pure matrices, such as in YAG (Y$_3$Al$_5$O$_{12}$ [**6**]), LuAG [**7, 8**], Sc$_2$O$_3$ [**9, 10, 11**] and Y$_2$O$_3$ [**9**], secondly, an increase in the wavelength of the main Yb^{3+} emission peak.

Starting from Y$_3$Al$_5$O$_{12}$ host an YSAG matrix is obtained by substituting Al^{3+} ions with Sc^{3+} ions. The role played by scandium can be summarized as it follows. The lattice structure is distorted owing to the larger ionic radius of scandium with respect to aluminum, resulting in a larger lattice constant [**12**]. This also modifies the crystal field and increases the splitting of the sublevels of the manifolds of Yb^{3+} [**13**]; whereas the overall energy difference of the barycenters of the manifold remains unchanged. These structural modifications determines a shift toward longer wavelengths of the main peaks of the emission spectrum of Yb^{3+}. Last but not least, the structural disorder induced by scandium ions affects both the absorption and the emission bands due to inhomogeneous broadening. Moreover it should be

noted that the balance between scandium and aluminum influences the lifetime of the Yb excited level and therefore the pump power level needed to reach the laser oscillation threshold; the lifetime is then a crucial parameter in order to build efficient laser systems.

In the experiment reported here, we studied a ceramic sample with composition 10 *at.%* Yb:Y$_3$Sc$_x$Al$_{(1-x)}$O$_{12}$ (x = 1.5). The sample was prepared by solid state reactive sintering under vacuum. This paper report a description of the spectroscopic properties of this material, (*i.e.* absorption and emission cross section spectra, excited laser level decay time), as well as the laser performance.

Experimental

The fabrication process of the ceramic is based on solid state vacuum sintering. Starting materials are high-purity (99.99%) commercial powders of Y$_2$O$_3$, Sc$_2$O$_3$, α-Al$_2$O$_3$ and Yb$_2$O$_3$; tetraethoxysilane (TEOS) and MgO powder were added as sintering aids. The powders are first mixed with ethanol, and milled for 12 h using high-purity corundum balls as milling bodies. The resulting slurry was then dehidrated (2h, 70 °C) and sieved using a 200-mesh screen. The sieved powder was then subjected to calcination to eliminate the organic compounds (4h, 600 °C). Pellets with

18 mm of diameter were obtained from the powders by a first phase of uniaxial pressing (46 MPa) followed by isostatic pressing (250 MPa), at room temperature. The sintering phase was carried out in a vacuum furnace with tungsten mesh-heaters (30h, 1820 °C). Finally, the samples were annealed in air to remove oxygen vacancy defects (20h, 1450 °C).

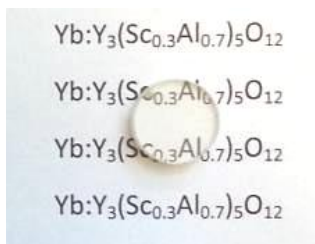**Fig. 1** reports a picture of the sample used in the experiment.

Fig. 1. 1.85-mm-lengh Yb:YSAG ceramic. The concentration of activators was 10*at.%* Yb^{3+}.

Concerning the spectroscopic characterization, we acquired the transmission spectrum of the sample in the range 200 nm – 1200 nm using a spectrophotometer (Model Lambda 1050, Perkin Elmer) (see **Fig. 2**).
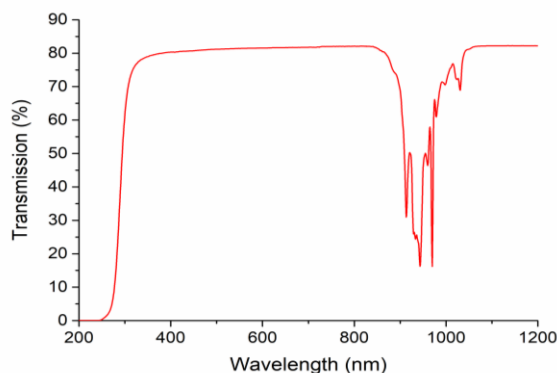

Fig. 2. Transmission spectrum (spectral resolution 1 nm). At 936 nm the transmission value is 66%.

The transmission spectrum allows calculating the absorption cross section and by the reciprocity method [**14**] the emission cross section, reported in **Fig. 3**.
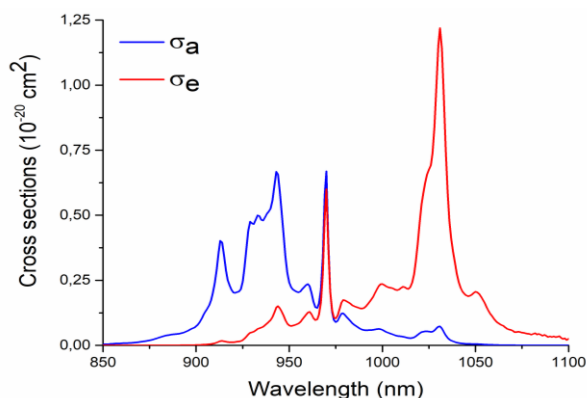

Fig. 3. Absorption (σ_a) and emission (σ_a) cross section spectra of the Yb^{3+}. The wavelength of the zero-phonon line is 969.7 nm; the peak emission cross section is $1.2 \times 10^{-21} cm^2$ at 1031 nm.

The upper laser level lifetime is measured by the pinhole method in order to compensate the radiation trapping effects [**15**]. The ceramic was excited by a nanosecond pulsed Ti:Sapphire laser. We measured a lifetime value of 966±6 μsec. Further information on the experimental apparatus can be found in [**16, 17**].

Fig. 4 reports the layout of the experiment for the characterization of the laser emission. The pump source is a fiber-coupled laser-diode (936 nm emission wavelength). The pump intensity distribution in the region of the focal plane is about Gaussian (waist radius ~95 μm at $1/e^2$). The sample was conductively cooled by a copper disk (with a central hole to let the laser beam pass through), where it was soldered using a layer of Indium. The copper mount was water-cooled at 17 °C. Two different campaigns of measurements were performed. In the former, the sample under test was pumped in *quasi*-CW regime (repetition rate 10 Hz, pump pulse duration 20 ms) with the purpose of limiting the thermal load experienced by the ceramic. In the latter, a true CW pumping regime was used to test the thermal behavior of the material.
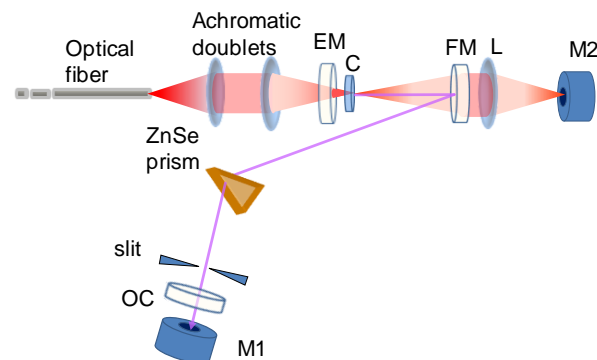

Fig. 4. Laser cavity layout used in the experiments. The folding angle is 20°. C: ceramic element under test; EM: pump injection mirror, flat; FM: Focusing Mirror (radius of curvature 100 mm); OC: Output Coupler mirror (flat); M1, M2: laser power meters, DM: Dichroic Mirror. The ZnSe prism and the slit were used only for the tuning measurements. The cavity length is 276 mm. The maximum pump power sent to the sample was 19.2 W.

The tuning of the laser emission wavelength was obtained by means of the intracavity zinc selenide prism (see **Fig. 4**). The prism has an apex angle 41.8° and is set to have incidence at the Brewster angle on both surfaces. We measured the lasing wavelength using a high resolution grating spectrometer with a CCD detector array (focal length 60 cm, overall resolution 0.4 nm).

Results and discussion

Fig. 5 reports the emitted power obtained with different levels of absorbed pump power, P_{abs}. The measurement was carried out in *quasi*-CW pumping regime; various output couplers (OC) were used with different values of transmission T, from 2.2% to 37.7%. We obtained the highest value of slope efficiency (η_s=67.8%) with the output coupler with transmission T=18.8%. The

maximum laser output was 6.3W, obtained with the output coupler with transmission T=18.8, at an emission wavelength of 1031 nm. The same output power and laser wavelength were obtained with the mirror with T=37.7%. The longest wavelength in free running lasing, *i.e.* λ_L=1051 nm, and the lowest laser threshold, *i.e.* P_{th}=0.74 W were measured with T=2.2%. The increase in the lasing wavelength observed by using the mentioned mirror is due to the *quasi*-three-level system behavior of the Yb^{3+}. When OCs with higher transmission are used, the cavity losses increase, thus requiring a higher fraction of the population in the upper laser level to sustain lasing; this in turns reduces the ground level absorption so that the effective gain spectrum moves to shorter wavelengths.
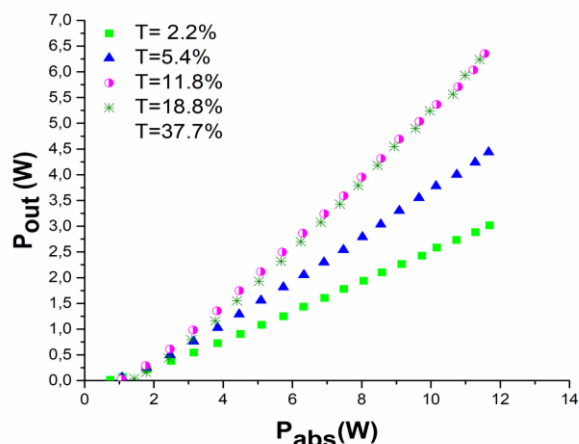

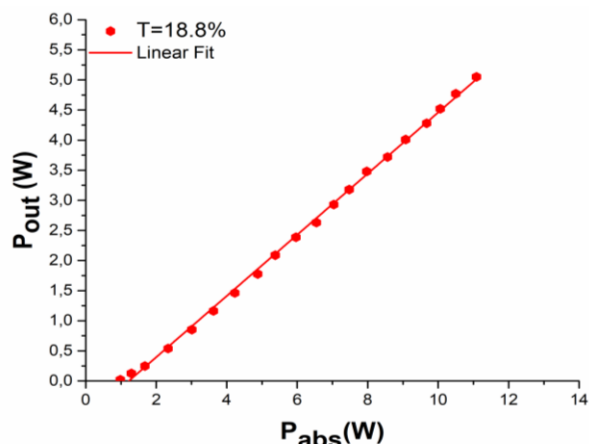**Fig. 5.** Laser peak power emission under *quasi*-CW pumping regime (10Hz, DF=20%) at 936 nm.

Fig. 6. CW laser output power measured by using T=18.8%.

Good results are achieved in CW pumping as well, see **Fig. 6**. The maximum output power was P_{out} = 5 W with a corresponding slope efficiency of η_s=52.7%. From these data we pointed out that the thermal load has only a moderate influence on the overall laser efficiency; in turn, we concluded that this ceramic shows high thermal quality.

Concerning the tunability of the sample we have measured the output power at several wavelengths; the tuning range spans from 991.5 nm to 1073 nm (overall

81.5 nm). Measurements were carried out in quasi-CW pumping regime as described above; the graph of **Fig. 7** reports the average output power. The data shows two main peaks at 1030 nm and 1050 nm. The corresponding output power is 118 mW and 89 mW, respectively. We note that the cutoff of the transmission curve of the EM limits the tuning range at short wavelengths. The sample was pumped with a peak incident power of 19.2 W, the absorbed pump power was P_{abs}= 11.7 W.
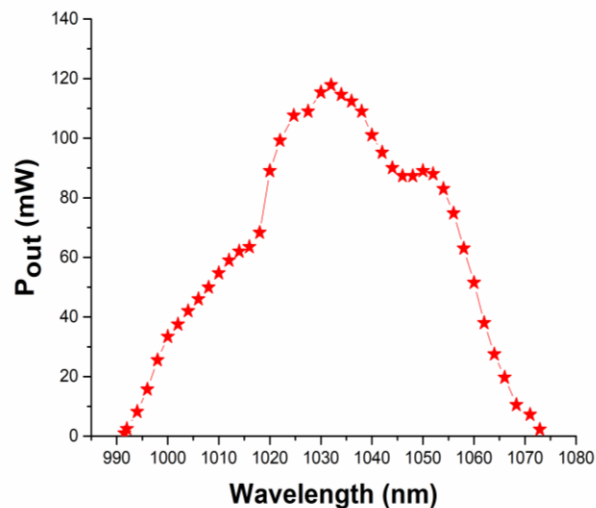

Fig. 7. *Quasi*-CW tuning curve. Pumping conditions: pump wavelength 936 nm, repetition rate 10Hz, pulse duration 20 ms. Reported values are the average power.

Conclusion

We have reported the spectroscopic characterization and the assessment of the laser emission properties of a transparent ceramic with composition $Y_3Sc_{1.5}Al_{3.5}O_{12}$ with 10 at. % Yb doping. The sample fabrication technique (reactive vacuum sintering) was also outlined.

The spectroscopic characterization addressed the absorption and emission cross section spectra and the lifetime of the Yb^{3+} excited level. In particular the mixed composition was found to have a significant impact on the emission spectrum, resulting in a substantial increase in the width of the main peak at 1031 nm (about 50% of the FWHM) in comparison with YAG.

Laser emission tests have shown high values of slope efficiency and output power and low laser pump threshold; this demonstrated the high optical quality of Yb:YSAG laser ceramics. Finally, the broad tuning range measured has confirmed the possibility to use this material in laser system able for achieving short pulses.

In future investigations we will assess the impact of the composition (in particular the ratio between Al and Sc) on the spectroscopic properties of the Yb and on the overall laser performance of this material, in order to get additional improvements and information.

References

1. Dong, J.; Ueda, K.; Kaminskii, A. A., *Opt. Express*, **2008**, *16*, 5241.
   DOI: 10.1364/OE.16.005241
2. Allik, T. H.; Morrison, C. A.; Gruber, J. B.; Kokta M. R., *Phys. Rev. B*, **1990**, *41*, 21.
   DOI: 10.1103/PhysRevB.41.21
3. Ikesue, A.; Aung, Y. L., *J. Am. Cer. Soc.*, **2006**, 89, 1936.
   DOI: 10.1111/j.1551-2916.2006.01043.x
4. Saikawa, J.; Sato, Y.; Taira, T.; Ikesue, A., *Opt. Mater.* **2007**, *29*, 1283.
   DOI: 10.1016/j.optmat.2006.01.031
5. Südmeyer, T.; Kränkel, C.; Baer C. R. E.; Heckl, O. H.; Saraceno, C. J.; Golling, M.; Peters, R.; Petermann, K.; Huber, G.; Keller, U., *Appl Phys B*, **2009**, *97*, 281.
   DOI: 10.1007/s00340-009-3700-z
6. Saikawa, J.; Sato, Y.; Taira, T.; Ikesue. A; Appl. *Phys. Lett.*, **2004**, *85*, 5845.
   DOI: 10.1063/1.1836019
7. Beil, K.; Fredrich-Thornton, S. T.; Tellkamp, F.; Peters, R.; Kränkel, C.; Petermann, K.; Huber, G., *Opt. Express*, **2010**, *18*, 20712.
   DOI: 10.1364/OE.18.020712
8. Pirri, A.; Vannini, M.; Babin, V.; Nikl, M.; Toci, G., *Las. Phys.*,**2013**, *23*, 095002.
   DOI: 10.1088/1054-660X/23/9/095002
9. Pirri, A.; Toci, G.: Patrizi, B.; Vannini, M., *IEEE J. Sel. Topics Quantum Electron.*, **2018**, *24*, 1602108.
   DOI: 0.1109/JSTQE.2018.2799003
10. Pirri, A.; Toci, G.; Vannini, M., *Opt. Lett.*, **2011**, *36*, 4284.
    DOI: 10.1364/OL.36.004284
11. Dai, Z.; Liu, Q.; Toci, G.; Vannini, M.; Pirri, A.; Babin, V.; Nikl, M.; Wang, W.; Chen, H.; Li, J., *J. Eur. Cer. Soc.*, **2018**, *38*, 1632.
    DOI: 10.1016/j.jeurceramsoc.2017.10.027
12. Kück, S.; Petermann, K.; Pohlmann, U.; Schönhoff, U.; Huber G., *Appl. Phys.*, **1994**, *58*, 153.
    DOI: 10.1007/BF01082351
13. Saikawa, J.; Sato, Y.; Taira, T.; Ikesue, A., *Appl. Phys. Lett.*, **2004**, *85*, 1898.
    DOI: 10.1063/1.1791339
14. DeLoach, L. D.; Payne, S. A.; Chase L. L.; Smith L. K.; Kway W. L; Krupke, W. F., *IEEE J. Quantum Electron.*, **1993**, *29*, 1179.
    DOI: 10.1109/3.214504
15. Kühn, H.; Fredrich-Thornton, S. T.; Kränkel, C.; Peters, R.; Petermann, K., *Opt. Lett.*, **2007**, *32,* 1908.
    DOI: 10.1364/OL.32.001908
16. Toci, G., *Appl. Phys. B*, **2012**, *106*, 63.
    DOI: 10.1007/s00340-011-4631-z
17. Toci, G.; Alderighi, D.; Pirri, A.; Vannini, M., *Appl. Phys. B*, **2012**, *106*, 73.
    DOI: 10.1007/s00340-011-4632-y